Carbohydrate Polymers 86 (2011) 797–805

Contents lists available at ScienceDirect

Carbohydrate Polymers

journal homepage: www.elsevier.com/locate/carbpol

Molecular characterization and hypoglycemic activity of a novel water-soluble polysaccharide from tea (*Camellia sinensis*) flower

Han Quan[a,b], Yu Qiong-yao[a,b], Shi Jiang[a,b], Xiong Chang-yun[a,b], Ling Ze-jie[a,b], He Pu-ming[a,b,*]

[a] Department of Tea Science, Zhejiang University, Hangzhou 310058, PR China
[b] Key Laboratory of Horticultural Plant Growth Development and Biotechnology of Ministry of Agriculture, Zhejiang University, Hangzhou 310058, PR China

ARTICLE INFO

Article history:
Received 25 January 2011
Received in revised form 8 May 2011
Accepted 18 May 2011
Available online 30 May 2011

Keywords:
Hypoglycemic
Tea flower
Thermo-gravimetric
Intrinsic viscosity
Laser light scattering

ABSTRACT

Two water-soluble polysaccharide fractions, coded as TFP-1 and TFP-2, were isolated from tea (*Camellia sinensis*) flower and further characterized using Ubbelohde viscometer, laser light scattering, particle size analyzer and thermo-gravimetric analyzer. Meanwhile, the intrinsic viscosities, weight-average molar mass, gyration radius and hydrodynamic radius for TFP-1 and TFP-2 were shown as follows: $[\eta] = 0.767$ and 0.207 dL/g, $M_w = 15.9 \times 10^4$ and 1.12×10^4 g/mol, $R_g = 37.2$ and 14.1 nm, $R_h = 44.8$ and 14.4 nm. Moreover, the shape-factor suggested the molecule morphology adopted a branched spherical shape in NaCl solution and the typical thermal behaviors of TFP-1 and TFP-2 were presented in analysis curves. Furthermore, research also presented the inhibitory effects against α-glucosidase and α-amylase. Moreover, continuous administration of TFP-2 with 75, 150 and 300 mg/kg/b.wt for 3 weeks caused a significant ($p < 0.01$) decrease in blood glucose levels of alloxan-induced diabetic mice. The results concluded that TFP-2 should be considered as a potential candidate for new antidiabetic agent.

1. Introduction

Nowadays, diabetes mellitus has been deemed as one of the major causes of the morbidity and mortality worldwide (Cline, Peterson, & Krassak, 1991). Additionally, there is no descent approach to treat it due to its variable causes. However, it has been discovered that a promising therapy for diabetes could be responsible for the disruption of carbohydrates through inhibition of the major digestive enzymes and α-amylase and α-glucosidase have been considered as potential targets to control diabetes (Jung, Matzke, & Stoltefus, 1996). Unfortunately, according to Larner (1985), synthetic hypoglycemic drugs, including insulin and other oral hypoglycemic agents such as biguanides, sulphonylureas, α-glucosidase (α-amylase as well) inhibitors can cause serious side effects. In that case, the demand for a new therapeutical agent without side effects originating from plants used in traditional medicines is urgent. Currently, polysaccharides, the biodegradable and environmentally friendly materials, have been extensively used in medical and pharmaceutical areas. Moreover, during the past decade, it is interesting to note that tea (*Camellia sinensis*) polysaccharides have been reported to exhibit hypoglycemic effects (Chen, Zhang, & Xie, 2005; Tadakazu, Tomoki, Hitoshi, Fumihisa, & Mistugu, 1998; Wang, Wang, Li, & Zhao, 2001; Zhou, Ding, & Wang, 1997).

Tea, a product originating from leaf and bud of *C. sinensis*, is the second most consumed beverage in the world, and it has become an important agricultural product. Cai (1979) considered that lower grade green tea has been used traditionally to control blood glucose (BG) in the body since the ancient time in China and Japan. Moreover, its hypoglycemic effects were most widely investigated and animal studies suggested that tea polysaccharide may help prevent the development of diabetes and postpone the progression once it has developed. However, there is but no detailed literature in terms of the effect of tea flower polysaccharide (TFP) on diabetes. In China, there is a phenomenon which cannot be neglected that the resources of tea flowers are abundant with the low utilization. Compared with tea leaves, tea flowers have similar chemical compositions and contain less caffeine but comparable amounts of total catechins and polysaccharide, furthermore, tea pollen was also characterized as an excellent protein resource (Yang, Xu, Jie, He, & Tu, 2007). With this in mind, tea flowers are of important application values as leaves. Additionally, TFP are the main effective components in tea flowers, accounting for a comparative large proportion, the studies and applications of TFP are also becoming intriguing. Nevertheless, until recently, few attempts have been devoted to polysaccharide from tea flower.

In our point of view, research on the molecular characteristics of the polymer molecules such as the molar mass, size, conformation and solvent quality in dilute solutions could provide insights into the physic-chemical behavior and indicate

* Corresponding author at: Department of Tea Science, Zhejiang University, 388 Yuhangtang Road, Hangzhou 310058, China. Tel.: +86 571 86041849; fax: +86 571 86971260.
E-mail addresses: pmhe@zju.edu.cn, puminghe@yahoo.com.cn (P.-m. He).

0144-8617/$ – see front matter © 2011 Elsevier Ltd. All rights reserved.
doi:10.1016/j.carbpol.2011.05.039

effective application of the biopolymer. The previous paper have obtained two homogeneous polysaccharide fractions which were separated from TFP by Sephadex G-100 column chromatography and have investigated into the structural features of fractions by HPGPC, rheometer, IR, NMR, AFM and SEM. Furthermore, the free radical-scavenging activities of TFP and two fractions have been elucidated (in press). In contrast, the excellent antioxidant ability of TFP-2 was attributed to its relatively low molecular weight, low apparent viscosity and particularity of chemical composition. As a result, based on the analysis shown above, the purpose of the present work is to gain an insight into the molecular characters of TFP fractions by viscometer, laser light scattering techniques, particle size analyzer and thermo-gravimetric analyzer. Moreover, the inhibitory effect of TFP-2 against digestive enzymes and hypoglycemic investigation on experimental diabetic mice were also evaluated afterwards, and the results provided the foundation for future pharmacological and biochemical studies.

2. Materials and methods

2.1. Chemicals and mice

Dry flowers of *C. sinensis* were offered by JingMao Tea Factory (JinHua, China) with uniform shape, color and florescence. The detailed procedure of isolation and purification of TFP fractions (coded as TFP-1 and TFP-2) were described previously (in press). Briefly, TFP-1 and TFP-2 are grayish powder which were isolated from tea flower by hot water extraction, ethanol precipitation, deproteinization by Sevag method (Sevag, Lackman, & Smolens, 1938), fractionation by Sephadex G-100, dried in vacuum and stored at 4 °C as required. The compositions of total sugars and total amino acids, uronic acid, protein and monosaccharides have already been tested. Alloxan, α-glucosidase and α-amylase were purchased from Sigma Chemical Co. (Saint Louis, USA). Reduced glutathione, p-nitrophenol-α-D-glucopyranose (pNPG), starch, Sephadex G-100 and OneTouch glucometer were obtained from HuaDong Medicine Co. (HangZhou, China). All of the other chemicals used were of analytical purity.

Eighty male ICR mice (2 months old, 20–24 g) were provided by ZheJiang Research Animal Center (Hangzhou, China). The mice were maintained at 24–26 °C on a 12/12 h light/dark cycle, and have been housed in plastic cages with free access to water and standard food. The study was conducted in accordance with the guide for care and use of laboratory animals and approved by the Animal Ethics Committee of China.

2.2. Physicochemical property of TFP fractions

Different solvents including distilled water, dilute acids, dilute bases, dilute salts and organic reagents (ethanol, acetone, ethyl acetate, and chloroform) were used to estimate the solubility of TFP fractions. Meanwhile, the specific rotation, $[a]_D$ of purified samples were measured at sodium *D* line 589 nm and 20 °C in 1 mg/mL aqueous solution using a P1030 digital polarimeter (JASCO, Japan). A 100 mm observation pipe was used to determine its optical rotation with sodium light. Specific rotatory power $[\alpha]_D{}^{20}$ was calculated as $[\alpha]_D{}^{20} = \alpha/LC$ (α, optical rotation; *L*, 1 dm; *C*, 0.001 g/mL).

2.3. Helix–coil transition assay

Helix–coil transition assay using Congo red dye was performed according to the reported method (Ogawa, Wanatabe, Tsurugi, & Ono, 1972) with slight modifications. TFP fractions (10 mg), dissolved in 2 mL distilled water, were mixed with 80 μM Congo red solution (2 mL). NaOH solution of 1 M was added drop by drop to make the final concentration of NaOH be 0.0, 0.1, 0.2, 0.3, 0.4 and 0.5 M, respectively. Additionally, visible spectra of mixture at various concentrations of NaOH were scanned on UV-2450 spectrophotometer (Shimadzu, Japan) at 400–800 nm and the maximum absorption wavelength was recorded, and distilled water, instead of TFP fractions, was mixed with Congo red and NaOH solution as control.

2.4. Intrinsic viscosity of TFP fractions

The conformation of polysaccharides in solutions, especially in aqueous solutions, could be investigated according to the theory of dilute polymer solutions. Inherent viscosity ($\ln \eta_r/c$) and specific viscosities (η_{sp}/c) were measured at 25 °C on conventional Ubbelohde type capillary viscometer (0.57 mm) for TFP fractions in 0.1 M NaCl solution. All the test solutions were maintained at a constant temperature within ±0.01 °C, and the flowing time was measured to a precision of 0.1 s. The kinetic energy correction was always negligible. Triplicate measurements were performed for each sample dilution. The intrinsic viscosity $[\eta]$ is a characteristic property of polysaccharide solution. Huggins Eq. (1) and Kraemer Eq. (2) were used to estimate the $[\eta]$ value by extrapolating to an infinite dilution:

$$\frac{\eta_{sp}}{C} = [\eta] + k'[\eta]^2 C \quad (1)$$

$$\frac{\ln \eta_r}{C} = [\eta] + k''[\eta]^2 C \quad (2)$$

where $[\eta]$ is the intrinsic viscosity, η_{sp} is the specific viscosity, η_r is the relative viscosity, k' is the Huggins coefficient, and k'' is the Kraemer coefficient. *C* is the sample concentration in 0.1 M NaCl solution.

2.5. Particle size analysis

One milligram of TFP fractions was dissolved in 50 mL of distilled water and vortexes for 3 min. 5 mL of polysaccharide solution was heating over 30 min in boiling water and then cooled to room temperature. The particle size analysis was evaluated using Brookhaven particle size analyzer (Brookhaven, New York, USA) with a focal length of 633 mm at 25 °C and plotted for size distribution using the 90Plus software supplied by the manufacturer.

2.6. TG thermal analysis

Thermo gravimetric analyzer (TGA) (DSCQ1000, Waters, Massachusetts, USA) was used to investigate the mass loss stages of TFP fractions. In the TGA experiment, the apparatus were continually flushed with nitrogen or air. TFP-1 and TFP-2 were dried in high vacuum at 25 °C at least 48 h and heated from 30 to 500 °C at a rate of 10 °C/min. The mass of the sample was less than 5 mg to avoid the possible temperature gradient inside the sample and ensure the kinetic control of the process (Blasi, Branca, Santoro, & Hernandez, 2001).

2.7. Light scattering measurements

2.7.1. Static light scattering experiments

The experiments were carried out in the angular range from 30° to 150° using BI-200SM static light scattering (SLS) system (Brookhaven, New York, USA) at 25 °C. The incident light was provided by a laser with a wavelength of 633 nm, and the scattered intensity was determined from different concentrations (0.05, 0.067, 0.1, 0.15 and 0.2 mg/mL) of polysaccharide solutions in 0.1 M NaCl solutions. These solutions were diluted from the stock solution of 1 g/L, which were filtered through 0.2 mm membrane before injection.

Zimm plot method was employed to characterize macromolecules in solution. In short, this method consisted in applying a beam of monochromatic light and measuring the intensity of the light scattered by the molecules for different angles of the incident beam (Ducela, Saulniera, Richardb, & Bourya, 2005). The objective of this analysis was to approach the conformation of the molecular chains (R_g) and the quality of the solvent (A_2) and to describe the supramolecular arrangements (Pezron, Djabourov, & Leblond, 1991). M_w, A_2 and R_g in dilute polymer solution were calculated based on the Rayleigh–Gans–Debye theory by Eq. (3):

$$\frac{K_c}{R_\theta} = \frac{1}{M_w}\left[1 + \frac{16\pi^2 n^2}{3\lambda^2} R_g^2 \sin^2\left(\frac{\theta}{2}\right)\right] + 2A_2C \quad (3)$$

where the optical constant $K = 4\pi^2 n^2 (dn/dc)^2/(N_A\lambda^4)$; dn/dc is refractive index increment; n is the solvent refractive index; θ is the observation angle; λ is the wavelength in vacuum of the laser, N_A is Avogadro's number and c is the concentration of the polymer solution. The Rayleigh ratio, $R_\theta = (I_\theta r^2/I_0)$, I_0 and I_θ are the intensity of the incident light and the scattered light; r is the distance from the light source to the measuring point. A plot of (K_c/R_θ) against $[\sin^2(\theta/2) + k_c]$ can be used to determine the molecular parameters (where k is an arbitrary constant). R_g, A_2 and M_w can be obtained by extrapolating the data to zero angle and concentration.

2.7.2. Dynamic light scattering experiments

The hydrodynamic radius R_h of polysaccharides in solution was measured by dynamic light scattering (DLS) spectrometer (BI-200SM) equipped with a BI-9000AT digital time correlator (Brookhaven, New York, USA) at 25 °C. DLS technique is a convenient method to figure out the size, shape, and dynamics of biological macromolecules and supramolecular assemblies, and to depict flow and other properties in physiological and biomedical situations (Pecora, 1985). A He–Ne laser (633 nm) was used as the light source at the angles range from 30° to 90° with an interval of 15°. The preparations of polysaccharides solutions have been mentioned in Section 2.7.1. In DLS, the Laplace inversion of each measured intensity–intensity time correlation function resulted in a characteristic line width distribution $G(\Gamma)$ (Zhang, Li, & Zhang, 2010). For a purely diffusive relaxation, the translational diffusion coefficient D at indefinite dilute was estimated from Γ by Eq. (4):

$$D = \lim_{\substack{q \to 0 \\ c \to 0}} \frac{\Gamma}{q^2} \quad (4)$$

where $q = (4\pi n/\lambda)\sin(\theta/2)$ with n, λ, and θ being the solvent refractive index, the wavelength in vacuum of the laser, and the observation angle, respectively; c is the concentration of the polymer solution. $G(\Gamma)$ can be further converted to a hydrodynamic radius (R_h) distribution using the Einstein–Stokes of Eq. (5):

$$R_h = \frac{k_B T}{6\pi\eta D} \quad (5)$$

where D is the diffusion coefficient, k_B, T, and η are the Boltzmann constant, the absolute temperature, and the solvent viscosity, respectively.

2.8. Inhibition effect on α-glucosidase in vitro

The α-glucosidase inhibitory activity of TFP-2 was measured according to the chromogenic method described by Chapdelaine, Tremblay, and Dube (1978) with some modifications. The substrate solution pNPG was prepared with 0.1 M phosphate buffer (pH 6.9). The reaction mixture was provided as follows: phosphate buffer, 2 mL; TFP-2 solution at different concentrations, 20 μL; 1 mg/mL reduced glutathione, 50 μL; 1 U/μL α-glucosidase, 20 μL. The mixed solution was incubated at 37 °C for 10 min. The enzymatic reaction was initiated by adding pNPG and the reaction mixture was incubated for another 30 min at 37 °C. The catalytic reaction was terminated by the addition of 10 mL of 0.1 M Na_2CO_3 solution, and resulting solution was measured at 400 nm. The reaction system without TFP-2 was used as blank and the system without α-glucosidase was used background. Experiments were analyzed in triplicate, and their mean values were noted. The inhibitory percentage was calculated by the following Eq. (6):

$$\text{Inhibition percentage } (\%) = 100 \times \left[1 - \frac{A_{sample} - A_{background}}{A_{blank}}\right] \quad (6)$$

2.9. Inhibition effect on α-amylase in vitro

Inhibition effect on α-amylase was based on the starch-iodine method that was originally described by Fuwa (1954) with slight modifications. Starch solution was prepared by dissolving 1 g of starch in 10 mL of distilled water, gently boiled, cooled and fixed to 100 mL with distilled water. The α-amylase solution was prepared by transferring 6 μL of α-amylase suspension (40 mg/mL) to 8 mL of phosphate buffer (pH 6.9). Briefly, 0.3 mL of α-amylase solution was added to a sample tube containing 0.3 mL of TFP-2 at different concentrations (substituted by TFP-2 in the case of background) and 0.6 mL of phosphate buffer. The mixture was incubated at 37 °C for 15 min. Aliquots (0.4 mL) of the mixture were transferred to sample tubes containing 3 mL of starch and 2 mL of phosphate buffer (pH 6.5) and the mixture was re-incubated for 45 min. 0.1 mL of the reaction mixture was withdrawn from each tube and added into 10 mL of iodine solution, then the resulting solution was monitored at 565 nm. Experiments were analyzed in triplicate, and their mean values were noted. The inhibitory percentage was calculated by the following Eq. (7):

$$\text{Inhibition percentage } (\%) = 100 \times \left[1 - \frac{(A_0 - A_t)_{sample}}{(A_0 - A_t)_{background}}\right] \quad (7)$$

where A_0 and A_t are the absorbance values of incubation time at $t = 0$ min and $t = 45$ min, respectively.

2.10. Acute toxicity studies

Healthy ICR mice fasted overnight were divided into three groups ($n = 10$) and were intragastric (i.g.) administrated with TFP-2 in increasing dose levels of 80, 400 and 2000 mg/kg/b.wt (Ghosh, 1984). The mice were continuously observed within 2 h for behavioral, neurological and autonomic profiles and after 24 and 72 h for any lethality or death (Turner, 1965).

2.11. Experiment design and biological analyses

Mice were adapted to diet for one week before the experiment conducted. After a 12 h fasting, 40 mice were induced with a single injection of alloxan prepared freshly at a dose of 260 mg/kg/b.wt. 24 h later after alloxan injection, whole blood samples were obtained from the tail vein of the overnight fasted mice and their glucose levels were tested by OneTouch glucometer. The mice with the BG levels over 11.1 mM were considered as diabetic and were used for the animal experiment. Mice were randomly divided into five experimental groups with ten mice in each group. The treatments have lasted for 3 weeks, and the body weights (BW) and BG levels were recorded weekly intervals when the mice were fasted overnight.

- Normal group: normal mice, received (i.g. distilled water).
- Control group: diabetic mice, received (i.g. distilled water).

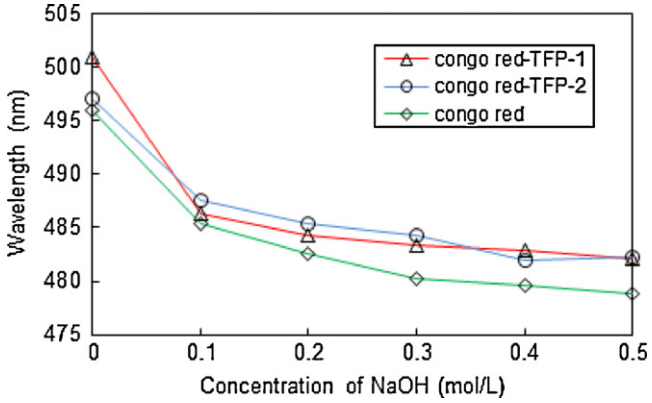

Fig. 1. Changes in absorption wavelength maximum of mixture of Congo red and TFP fractions at various concentrations of NaOH.

- L-TFP group: diabetic mice, received (i.g. TFP-2 75 mg/kg/b.wt).
- M-TFP group: diabetic mice, received (i.g. TFP-2 150 mg/kg/b.wt).
- H-TFP group: diabetic mice, received (i.g. TFP-2 300 mg/kg/b.wt).

2.12. Statistical analyses

All the results were expressed as mean ± S.E. for ten mice in each group. And the statistical analysis was carried out using one-way ANOVA followed by Tukey post hoc test. The criterion for statistical significance was $p < 0.05$.

3. Results

3.1. Characterization of TFP fractions

With the aim to obtain high-purity and homogeneity polysaccharide products for stable functional property, the TFP were purified by Sephadex G-100 gel permeation chromatography into different fractions according to their molecular size. Each fraction was eluted as a single symmetrical peak, which indicated that TFP-1 and TFP-2 were homogeneous fractions with different molecular sizes. Both of the two products were soluble in water, dilute acids, dilute bases and dilute salts, while insoluble in organic reagents. The $[\alpha]_D^{20}$ values of TFP-1 and TFP-2 were 51.8 and 17.6.

3.2. Identification of helix–coil transition

The conformational behavior of polysaccharide, if it possessed triple helical structure, could be evaluated from the shift in the absorption wavelength maximum when Congo red dye was added to sample at various concentrations of alkali (Qiao et al., 2010). Fig. 1 displays the variation curves of absorption wavelength maximum of mixture at various concentrations of NaOH solution, the curves decreased gradually with the increasing of NaOH concentration and no characteristic variance of triple helical structure were detected in TFP fractions.

3.3. Intrinsic viscosity of TFP fractions

The intrinsic viscosity is a measure of the hydrodynamic volume occupied by macromolecules in a dilute solution and very sensitive to the extension of polymer chains. Both of the Huggins and Kraemer functions were used to determine the $[\eta]$ of the polysaccharide molecules. It was carried out by extrapolating the plots to infinite dilution where the effects of intermolecular interactions were absent. The Huggins parameter (k') and Kraemer parameter (k'') were considered as an indicator of the interactions between solvent molecules and the macromolecular species in solution (Bohdanecky & Kovar, 1982; Morris, 1989). k' usually had values between 0.3 and 0.8, with values of 0.3–0.4 for a polymer in good solvents and 0.5–0.8 for polymers in θ solvents. For values above 0.8, aggregation of the macromolecules was likely to have occurred (Doublier & Cuvelier, 1996). At the same time, negative values for k'' indicate good solvents and positive values, poor ones (Gillespie, 1964; Oliveira, Andrade, & Delpech, 1991). Fig. 2 describes Huggins and Kraemer plots (η_{sp}/C and $\ln \eta_r/C$ versus C) for TFP fractions in 0.1 M NaCl aqueous solution, the intrinsic viscosity $[\eta]$ and Huggins constant (k') were 0.767 dL/g and 0.342 for TFP-1, while 0.207 dL/g and 0.395 for TFP-2.

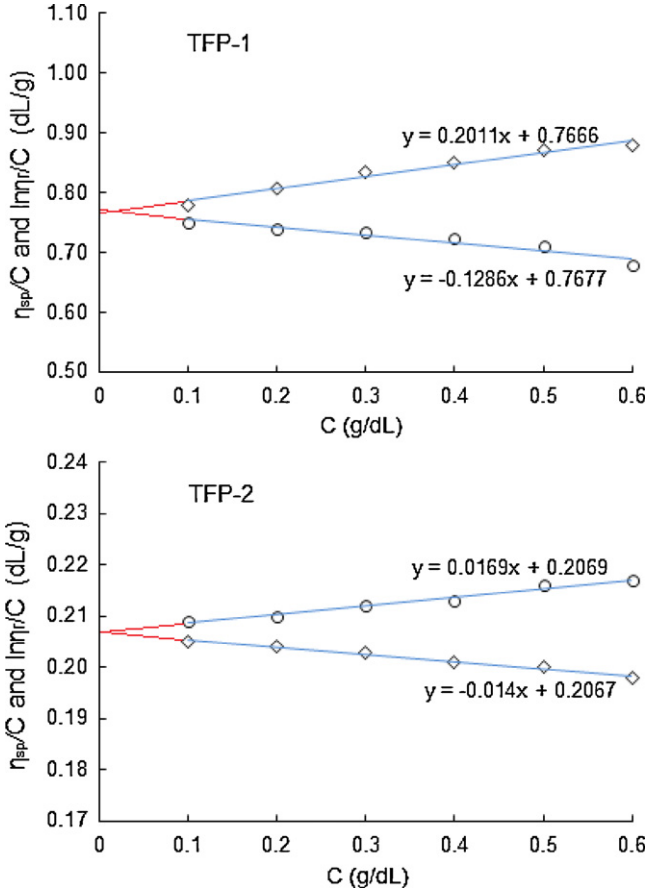

Fig. 2. Huggins and Kraemer plots for the TFP fractions in 0.1 M NaCl aqueous solution at 25 °C.

3.4. Analysis of the particle size

The particle size distribution, which was presented as volume fraction versus particle diameter, is provided in Fig. 3. It appeared that TFP-1 had diameters in the range of the 50–170 nm before heated, while TFP-2 was in the range of the 5–100 nm. TFP-1 solution by heat treatment produced bigger size particles (100–380 nm) with relatively wide distribution than that before heated (Fig. 3B), and a distinct population of big size particles (50–250 nm) in heated TFP-2 was also apparent from Fig. 3D. After the heat treatment, the effective diameter of TFP-1 and TFP-2 were approximately 110–200 nm and 40–110 nm, respectively. For both of the polysaccharide fractions, a certain degree of particle coagulation was observed during the heat treatment, and the big size particles might be attributed to multimer of particles. As a result, this phenomenon supposed that TFP fractions have a certain amount of hydroxyl

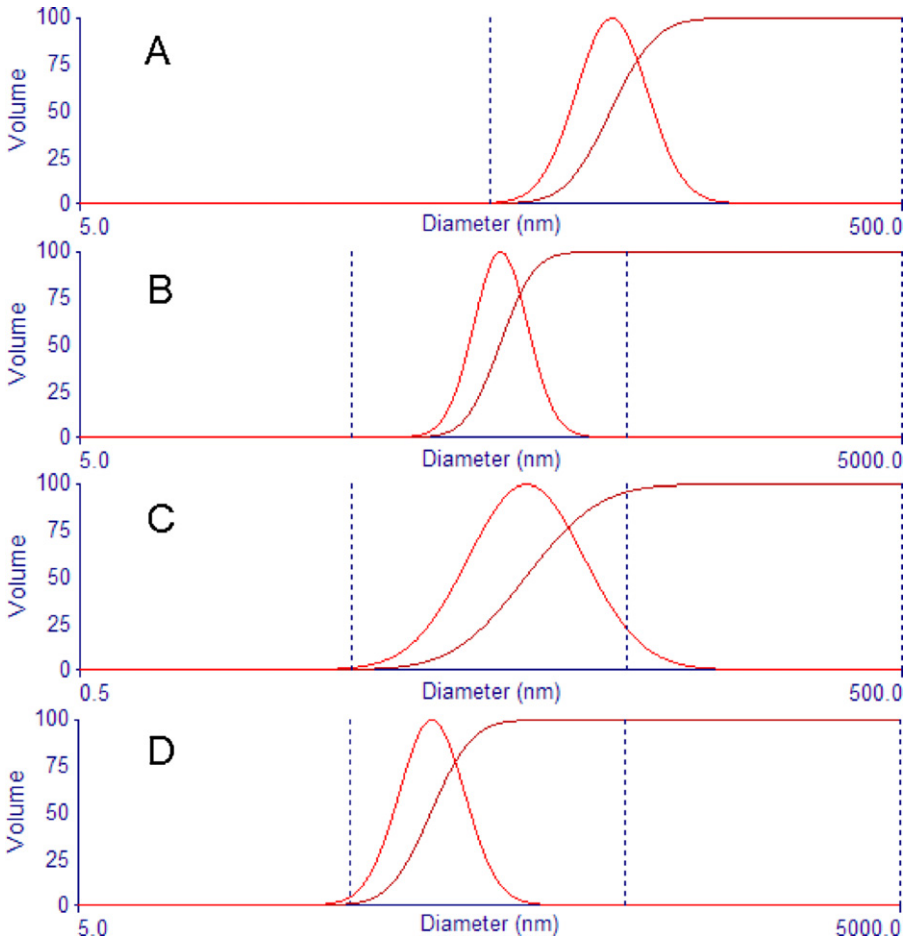

Fig. 3. Particle size volume distributions of TFP fractions. (A) TFP-1 before heated; (B) TFP-1 after heated; (C) TFP-2 before heated; and (D) TFP-2 after heated.

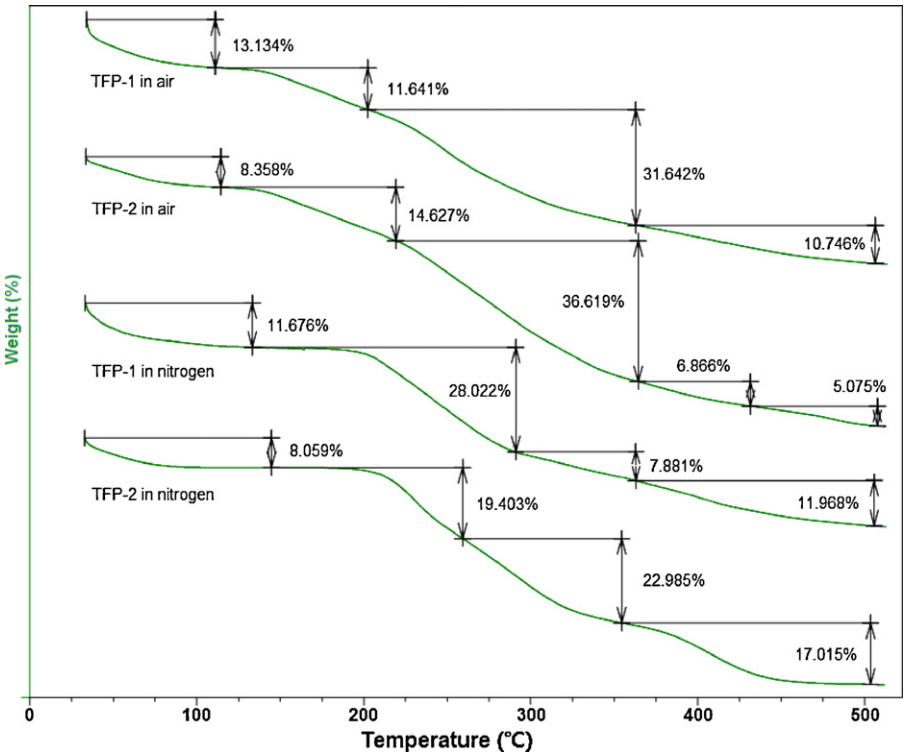

Fig. 4. The TG curves of TFP fractions at 10 °C/min. (A) TFP-1 in air; (B) TFP-2 in air; (C) TFP-1 in nitrogen; and (D) TFP-2 in nitrogen.

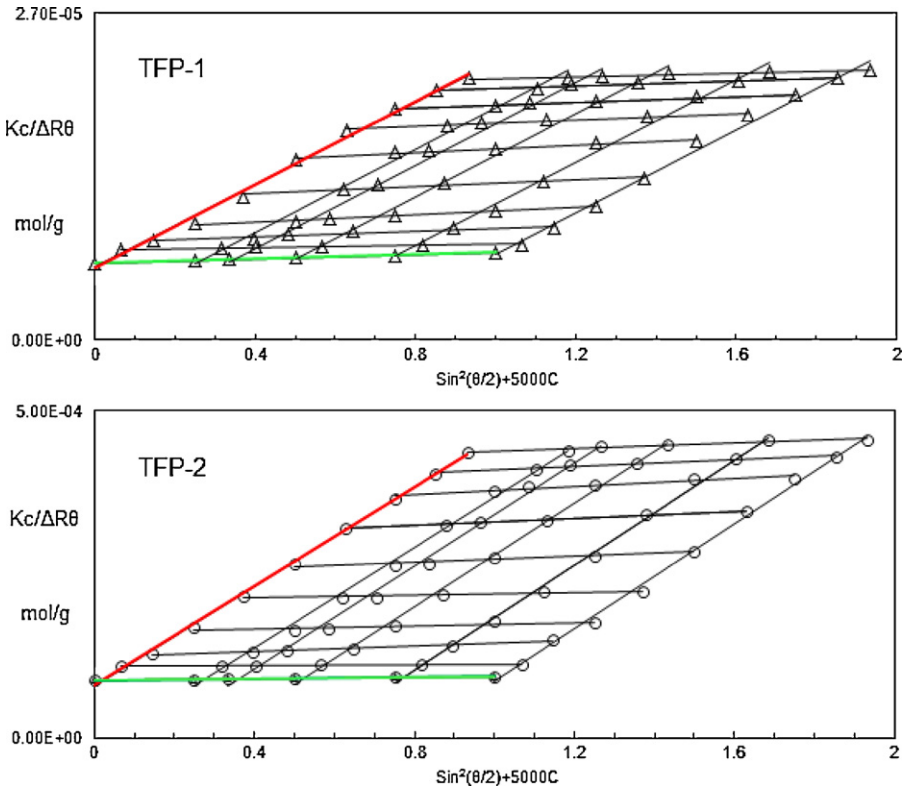

Fig. 5. Static light scattering data illustrated in a Zimm plot obtained from TFP-1 and TFP-2 in 0.1 M NaCl solutions.

groups and carboxyl groups, which entangled with each other. The aggregated polysaccharide molecules unfolded by heating in boiling water and reassembled when temperature recovered, and the increased interaction which are largely responsible for the formation of the polysaccharide molecules leads to the big size particles in aqueous solution.

3.5. TG analysis of TFP fractions

Marinho-Soriano and Bourret (2005) argued that the applicability of the polysaccharide was mainly dependent on its thermal and rheological behavior besides its chemical properties. In the 30–500 °C temperature range (Fig. 4), TFP-1 and TFP-2 synthesized the typical parameters of TGA curves. The thermal decomposition proceeded mainly in two steps: the first one with a low rate of decomposition while the second one with a relative rapid decomposition rate. TFP-1 and TFP-2 exhibited weight loss of 13.13% and 8.36%, respectively, which could be ascribed to the release of physically absorbed water or structural water and also perhaps due to the elimination of some side group. The anhydrous TFP-1 and TFP-2 were thermally stable up to 120 °C. An "abrupt mass loss stage" for TFP-1 (43.28%) and TFP-2 (51.24%) was observed within the temperature gap from 120 to 360 °C, where TFP-1 and TFP-2 depolymerized by the rupture of C–O and C–C bonds in the ring units. Decomposition resulted in the evolution of CO, CO_2 and H_2O, and formation of polynuclear aromatic and graphitic carbon structures (Zamora et al., 2002), the residual yield at 500 °C were about 32.8% and 26.5%. On the other hand, TFP-1 and TFP-2 had a lesser (35.90% and 42.39%) decline of the mass loss from 180 to 350 °C in nitrogen (Fig. 4). Comparatively the initial time of mass loss stage in air (180 and 120 °C), a slight increase of resistance to thermal degradation was observed in nitrogen, which could probably be attributed to the thermo-oxidative decomposition of TFP fractions in air.

3.6. Laser light scattering measurements

The M_w, R_g and A_2 extracted from the Zimm plots from TFP-1 and TFP-2 are illustrated in Fig. 5. However, it could be noted from the Zimm plots that the angular dependence of the scattered light did not change systematically with the decreasing concentration of the polymer, which could be deemed that there is no detectable conformation change of the molecules upon dilution. The M_w values obtained from SLS measurement were in fair agreement with the previous result obtained from HPGPC. From the Zimm plot, TFP-2 had a much lower molecular weight (1.12×10^4 g/mol) compared with the TFP-1 (15.9×10^4 g/mol). The R_g value was usually a measure regarding how far from the center of mass and how the mass of the polymer chains was concentrated. Smaller R_g value reflected polymer chains with more compact conformation when R_h remains constant. The R_g for both of the samples was 37.2 and 14.1 nm. By the application of Stokes–Einstein equation, the hydrodynamic radiuses R_h were calculated to be 44.8 and 14.4 nm for TFP-1 and TFP-2, respectively. In this case, the second virial coefficient A_2, an important parameter for a polymer–solvent system, could be deemed as positive and small for both samples, consequently, it indicated that polymer molecules mainly interact with solvent molecules. In addition, A_2 was lower for TFP-1 (4.85×10^{-3} mol mL/g^2) than TFP-2 (2.35×10^{-2} mol mL/g^2), and this behavior showed a higher interaction for TFP-2 molecules with the solvent.

3.7. Analysis of the molecular shape

Because the static and hydrodynamic dimensions are varied characteristically with the structure of the macromolecules, a combination of those two dimensions may provide qualitative information on the architecture of the macromolecules in detail. A dimensionless shape-factor ρ, which had been proven to be a

fairly sensitive measure of the shape of polymer molecules, was obtained from the ratio according to Eq. (8):

$$\rho = \frac{R_g}{R_h} \quad (8)$$

In terms of the theory, ρ was about 0.7–0.8 for a uniform sphere; 1.0–1.1 for a loosely connected hyperbranched chain or aggregate, 1.5–1.8 for a linear flexible random coil chain in a good solvent, and that was more than 2.0 for an extended rigid chain (Kajiwara & Burchard, 1984; Konishi, Yoshizak, & Yamakawa, 1991; Niu, Liaw, Sang, & Wu, 2000). Large ρ values indicated open structures and low ρ values rather dense structures, as were encountered for stiff chains and globular structures, respectively (Burchard, 1994). The factor ρ was not dependent on the bond length and the degree of polymerization but is a function of the branching density (branching causes ρ to decrease), the polydispersity (increase in polydispersity causes ρ to increase) and the inherent flexibility of the subchains (increase chain flexibility causes ρ to decrease) (Adolphi & Kulicke, 1997; Burchard, Schmidt, & Stockmayer, 1980). From the results of laser light scattering measurements, the ρ values were calculated to be 0.83 and 0.98, respectively, which were a little higher than the theoretical value for a homogeneous sphere (0.78) (Nichifor, Lopes, Carpov, & Melo, 1999) and lower than that of loosely connected hyper-branched chain (1.0–1.1), but in good agreement with the predicted value for a highly branched spherical shape molecule. These results further confirmed that TFP-1 and TFP-2 existed almost as a branched spherical shape in 0.1 M NaCl aqueous.

With the aim to further prove the conjecture mentioned above, the Mark–Houwink empirical Eq. (9) was used to validate the molecular morphology:

$$[\eta] = kM_w^{\alpha} \quad (9)$$

The Mark–Houwink equation could be established as $[\eta] = 0.206 \times M_w^{0.494}$ based on the respective M_w and intrinsic viscosity $[\eta]$ values of TFP-1 and TFP-2. The character constant α had an intimate relationship with the rigidity degree and solvation ability of the molecular chain and its value depended on the polymer solution system property and polymer chain structure. In general, α exponent with a rough value of 0.5 suggested that the polymer molecules behaved as a sphere, and a value from 0.6 to 0.8 indicated a flexible chain, while the value over 1 meant an elongated rod. Likewise, the experimental result of 0.494 for TFP also interpreted that the TFP molecule existed as spherical conformation in solution (Gabriela & Walther, 1995).

3.8. Inhibitory effects against α-glucosidase and α-amylase activities in vitro

Fig. 6 depicts the dose-dependent curves of inhibitory effects against α-glucosidase and α-amylase. It was found that the inhibitory effect of TFP-2 against α-glucosidase increased rapidly with the increasing concentration of TFP-2. The TFP-2 (2.0 mg/mL) presented an obviously inhibitory effect against α-glucosidase with the inhibitory rate of 57.2%. As illustrated in the Fig. 6, the inhibitory percentage of TFP-2 at 2.0 mg/mL for α-amylase was 29.5% while the inhibitory percentages of TFP-2 against α-amylase were inferior at every concentration point (0.2–2.0 mg/mL) compared with α-glucosidase.

3.9. Changes of body weights and blood glucose levels in diabetic mice after TFP-2 administration

The acute toxicity study of TFP-2 revealed that there was no lethality or any toxic reactions found at any of the doses selected until the end of the experiment period. Fig. 7 describes the effect

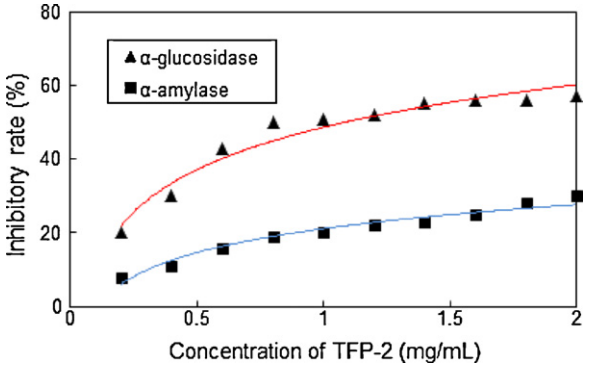

Fig. 6. Inhibitory effect of TFP-2 on α-glucosidase and α-amylase in vitro.

of TFP-2 on BW of severe diabetic mice. At the beginning of the study BW was not significantly ($p > 0.05$) different between TFP treated and diabetic control group. After 3 weeks, a significant decrease ($p < 0.01$) of 7.9% in BW was registered in the case of control group mice while in the treated groups the weight loss (5.3%, 4.1% and 3.8%) were generally reversed. The ability of TFP-2 to protect BW loss seemed to be as a result of its ability to reduce hyperglycemia. The BG levels of different treated groups are presented in Fig. 8. The alloxan-induced diabetic mice presented a significant increase ($p < 0.01$) in fasting BG in comparison to the normal group. Meanwhile, compared with the control group, the administration of TFP-2 for 3 weeks in diabetic mice caused a significant dose-dependent decrease in BG levels ($p < 0.01$) by 29.5%, 39.6% and 42.2%, respectively. Moreover, it did not normalize the BG levels completely as it remained higher than the normal mice.

4. Discussion

Considering the previous reports (Liu, Liu, & Wang, 1999), there are several main mechanisms for polysaccharides to act on the BG level, to decrease the content of liver glycogen, to stimulate the release of insulin, to influence the activities of digestive enzymes, or to exert beneficial effects in attenuating oxidative stress. However, commonly the onset of these functions was available when polysaccharide was given by intraperitoneal route but no obvious effect by oral route in diabetic mice. The bioactivities of the polysaccharide in vivo could be influenced by many factors including chemical

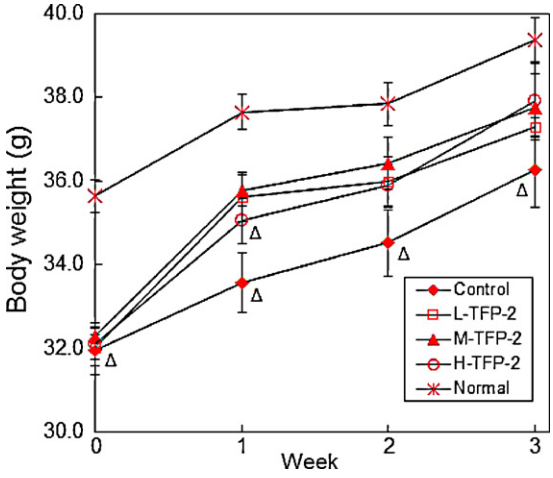

Fig. 7. Effect of TFP-2 on BW in alloxan-induced diabetic mice. Values are expressed as mean ± S.E. for ten mice in each group. One-way ANOVA with Tukey post hoc test was used to calculate statistical significance. (△) $p < 0.01$ as compared to the normal group.

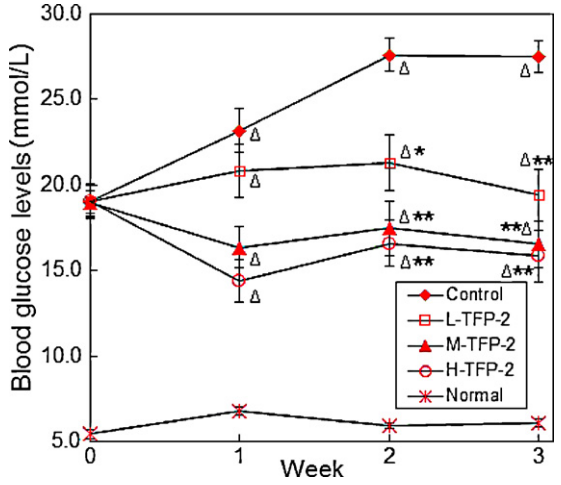

Fig. 8. Effect of TFP-2 on BG levels in alloxan-induced diabetic mice. Values are expressed as mean ± S.E. for ten mice in each group. One-way ANOVA with Tukey post hoc test was used to calculate statistical significance. (△) $p < 0.01$ as compared to the normal group; (*) $p < 0.05$ as compared to the control group; (**) $p < 0.01$ as compared to the control group.

components, molecular weight, configuration and position of glycosidic linkages, branching points and sequence of monosaccharide (Zhang, Cui, Cheung, & Wang, 2007), even the dose, time and route for administration. Despite that TFP-2 was administered intragastrically, the activity of TFP-2 significantly decreased BG level in diabetic mice. Furthermore, the observed inhibitory effects of TFP-2 on α-amylase and α-glucosidase were attributed to its especial affinity to target enzymes. Accordingly, it is hypothesized that the physical properties of TFP-2 (e.g. low viscosity, low M_w and morphology of branched spherical shape) endowed with a facility to pass through organizational barriers to enter the interior of the cell or attach to the receptors (Sun, Wang, Shi, & Ma, 2009).

The strategy of therapeutic approaches for diabetes mainly focuses on reducing fluctuations in BG levels. One of them is to decrease the postprandial hyperglycemia by retarding absorption of glucose by inhibition of carbohydrate-hydrolyzing enzymes, such as α-amylase and α-glucosidase (Bhandari, Jong-Anurakkun, Hong, & Kawabata, 2008). Currently, α-glucosidase inhibitors are currently employed for diabetes as oral hypoglycemic agents due to the capability of inhibiting the degradation of disaccharide to monosaccharide. The α-amylase inhibitors could retard starch digestion rate of food and restrain the increase of postprandial BG levels. Alloxan is a chemical commonly used to generate diabetic animals for its ability to destroy insulin-producing β-cells. It is generally accepted that free radicals, especially superoxide radicals, hydroxyl radicals or alloxan radicals induced by alloxan initiate damage that ultimately leads to β-cell death and hypoinsulinemia (Janjic et al., 1999; Murata, Imada, Inoue, & Kawanishi, 1998; Rahimi, Nikfar, Larijani, & Abdollahi, 2005). As is widely known, diabetics and experimental animal models reveal high oxidative stress due to persistent and chronic hyperglycemia, thereby deplete the activity of antioxidative defense system and promote free radical generation (Baynes & Thorpe, 1996). Oxidative stress might constitute a focus on multiple therapeutic interventions, and for therapeutic synergy. Antioxidants have been acknowledged to alleviate the destruction of β-cells (Murthy, Shipp, Hanson, & Shipp, 1992; Slonim, Surber, Page, Sharp, & Burr, 1983) by inhibiting the peroxidation chain reaction and thus they may provide protection against the development of diabetes. Previously, we demonstrated that TFP-2 possessed prominent scavenging activities against superoxide radical, hydroxyl radical and DPPH radical in vitro (in press). Considering all these facts, we assumed that TFP-2 has a potential effect to counteract the negative effect of the oxidative stress and inhibits the activities of major digestive enzymes, which could be partially responsible for TFP-2's significant hypoglycemic property. Thereby, TFP-2, a α-amylase, α-glucosidase inhibitor and antioxidant, which were more effective with less side effects, appeared to become one of the research hotspots as hypoglycemic agents. The comprehensive investigations on the hypoglycemic mechanisms of TFP-2 are undergoing and would be reported in due course.

5. Conclusions

As discussed above, the characterization of polysaccharide fractions obtained from tea flower were ascertained with viscometer, laser light scattering technique, particle size analyzer and thermogravimetric analysis. Experimental data have provided evidences that the M_w, $[\eta]$, R_g and R_h of were 15.9×10^4 g/mol, 0.767 dL/g, 37.2 and 44.8 nm for TFP-1, while 1.12×10^4 g/mol, 0.207 dL/g, 14.1 and 14.4 nm for TFP-2. The molecular conformation outlines as a spherical polymer with branch in 0.1 M NaCl solution. Furthermore, the typical thermal behaviors of TFP fractions were also presented in analysis curves. The potential inhibitory effects of TFP-2 against α-glucosidase and α-amylase increased rapidly with the increasing dose in vitro. In addition, those data also have revealed that continuous administration of TFP-2 for 3 weeks possessed notable hypoglycemic activity in dose-dependent manners. Consequently, it could been concluded that TFP-2 should be considered as a candidate for further studies on diabetes.

Appendix A. Supplementary data

Supplementary data associated with this article can be found, in the online version, at doi:10.1016/j.carbpol.2011.05.039.

References

Adolphi, U., & Kulicke, W. M. (1997). Coil dimensions and conformation of macromolecules in aqueous media from flow field-flow fractionation/multi-angle laser light scattering illustrated by studies on pullulan. *Polymer*, *38*, 1513–1519.
Baynes, J. W., & Thorpe, S. R. (1996). The role of oxidative stress in diabetic complications. *Current Opinion in Endocrinology*, *3*, 277–284.
Bhandari, M. R., Jong-Anurakkun, N., Hong, G., & Kawabata, J. (2008). α-Glucosidase and α-amylase inhibitory activities of Nepalese medicinal herb Pakhanbhed (*Bergenia ciliata*, Haw.). *Food Chemistry*, *106*, 247–252.
Blasi, C. D., Branca, C., Santoro, A., & Hernandez, E. G. (2001). Pyrolytic behavior and products of some wood varieties. *Combustion and Flame*, *124*, 165–177.
Bohdanecky, M., & Kovar, J. (1982). *Viscosity of polymer solutions*. Netherlands: Elsevier Scientific Publishing Company.
Burchard, W. (1994). Light scattering techniques. In S. B. Ross-Murphy (Ed.), *Physical techniques for the study of food biopolymers* (pp. 151–213). United Kingdom: Chapman & Hall.
Burchard, W., Schmidt, M., & Stockmayer, W. H. (1980). Information on polydispersity and branching from combined quasi-elastic and integrated scattering. *Macromolecules*, *13*, 1265–1272.
Cai, H. E. (1979). Reports of the treatment of diabetes by tea with integrated traditional Chinese and Western medicine. *Tea Research Bulletin*, *11*, 58–59.
Chapdelaine, P., Tremblay, R. R., & Dube, J. Y. (1978). *p*-Nitrophenyl-aglucopyranoside as substrate for measurement of maltase activity in human semen. *Clinical Chemistry*, *24*, 208–211.
Chen, H. X., Zhang, M., & Xie, B. J. (2005). Components and antioxidant activity of polysaccharide conjugate from green tea. *Food Chemistry*, *90*, 17–21.
Cline, G. W., Peterson, F., & Krassak, M. (1991). Impaired glucose transport as a cause decreased insulin stimulated muscle glycogen synthesis in Type 2 diabetes. *New England Journal of Medicine*, *3431*, 240.
Doublier, J. L., & Cuvelier, G. (1996). Gums and hydrocolloids: Functional aspects. In A. C. Eliasson (Ed.), *Carbohydrates in food* (pp. 283–318). United States of America: Marcel Dekker, Inc.
Ducela, V., Saulniera, P., Richardb, J., & Bourya, F. (2005). Plant protein-polysaccharide interactions in solutions: Application of soft particle analysis and light scattering measurements. *Colloids and Surfaces B: Biointerfaces*, *41*, 95–102.
Fuwa, H. (1954). A new method of micro-determination of amylase activity. *Journal of Biochemistry*, *41*, 583–603.
Gabriela, G., & Walther, B. (1995). Macromolecules starch fractions as examples for nonrandomly branched macromolecules. 1. *Dimensional Properties*, *289*, 2362–2370.

Ghosh, M. N. (1984). *Fundamentals of experimental pharmacology*. Calcutta: Scientific Book Agency.
Gillespie, T. (1964). The use of viscosity to assess molecular entanglement in dilute solutions. *Journal of Polymer Science Part C*, *3*, 31.
Janjic, D., Maechler, P., Sekine, N., Bartley, C., Annen, A. S., & Wollheim, C. B. (1999). Free radical modulation of insulin release in INS-1 cells exposed to alloxan. *Biochemical Pharmacology*, *57*, 639–648.
Jung, B., Matzke, M., & Stoltefus, J. (1996). Chemistry and structure activity relationship of glucosidase inhibitors. In J. Kuhlman, & W. Puls (Eds.), *Handbook of experimental pharmacology: Oral antidiabetics* (pp. 411–467). Berlin: Springer.
Kajiwara, K., & Burchard, W. (1984). Rotational isomeric state calculations of the dynamic structure factor and related properties of some linear chains. 1. The $\rho = \langle S_2 \rangle^{1/2} \langle R_H^{-1} \rangle$ parameter. *Macromolecules*, *17*, 2669–2673.
Konishi, T., Yoshizak, T., & Yamakawa, H. (1991). On the universal constants ρ and Φ of flexible polymers. *Macromolecules*, *24*, 5614–5622.
Larner, J. (1985). *The pharmacological basis of therapeutics* (7th edition). New York: Macmillan.
Liu, C., Liu, Z. Y., & Wang, Q. M. (1999). Studying progress in herbal polysaccharides on hypoglycemic activities. *Journal of Anhui TCM College*, *18*, 83–85.
Marinho-Soriano, E., & Bourret, E. (2005). Polysaccharides from the red sea-weed Gracilaria dura (Gracilariales, Rhodophyta). *Bioresource Technology*, *96*, 379–382.
Morris, E. R. (1989). Polysaccharide solution properties: Origin, rheological characterization and implications for food systems. In R. P. Millane, J. N. BeMiller, & R. Chandrasekaran (Eds.), *Frontiers in carbohydrate research, 1: Food applications* (pp. 132–163). London: Elsevier Applied Science.
Murata, M., Imada, M., Inoue, S., & Kawanishi, S. (1998). Metal-mediated DNA damage induced by diabetogenic alloxan in the presence of NADH. *Free Radical Biology and Medicine*, *25*, 586–595.
Murthy, V. K., Shipp, J. C., Hanson, C., & Shipp, D. M. (1992). Delayed onset and decreased incidence of diabetes in BB rats fed free radical scavengers. *Diabetes Research and Clinical Practice*, *18*, 11–16.
Nichifor, M., Lopes, A., Carpov, A., & Melo, E. (1999). Aggregation in water of dextran hydrophobically modified with bile acids. *Macromolecules*, *32*, 7078–7085.
Niu, A., Liaw, D. J., Sang, H. C., & Wu, C. (2000). Light-scattering study of a zwitterionic polycarboxybetaine in aqueous solution. *Macromolecules*, *33*, 3492–3494.
Ogawa, K., Wanatabe, T., Tsurugi, J., & Ono, S. (1972). Conformational behavior of agel-forming (1 → 3)-β-glucan in alkaline solution. *Carbohydrate Research*, *23*, 399–405.
Oliveira, C. M. F., Andrade, C. T., & Delpech, M. C. (1991). Properties of poly (methyl methacrylate-g-propylene oxide) in solution. *Polymer Bulletin*, *26*, 657.
Pecora, R. (1985). *In dynamic light scattering*. New York/London: Plenum Press.
Pezron, I., Djabourov, M., & Leblond, J. (1991). Conformation of gelatin chains in aqueous solutions: 1. A light and small-angle neutron scattering study. *Polymer*, *32*, 3201.
Qiao, D. L., Liu, J., Ke, C. L., Sun, Y., Ye, H., & Zeng, X. X. (2010). Structural characterization of polysaccharides from Hyriopsis cumingii. *Carbohydrate Polymers*, *82*, 1184–1190.
Rahimi, R., Nikfar, S., Larijani, B., & Abdollahi, M. (2005). A review on the role of antioxidants in the management of diabetes and its complications. *Biomedicine and Pharmacotherapy*, *59*, 365–373.
Tadakazu, T., Tomoki, U., Hitoshi, K., Fumihisa, Y., & Mistugu, M. (1998). The chemical properties and functional effects of polysaccharides dissolved in green tea infusion. *Nippon Shokuhin Kagaku Kogaku Kaishi*, *45*, 270–272.
Turner, M. A. (1965). *Screening methods in pharmacology*. New York: Academic Press.
Sevag, M. G., Lackman, B. D., & Smolens, J. (1938). The isolation of the components of streptococcal nucleoproteins in serologically active form. *Journal of Biological Chemistry*, *124*, 425–436.
Slonim, A. E., Surber, M. L., Page, D. L., Sharp, R. A., & Burr, I. M. (1983). Modification of chemically induced diabetes in rats by vitamin E. Supplementation minimizes and depletion enhances development of diabetes. *Journal of Clinical Investigation*, *71*, 1282–1288.
Sun, L. Q., Wang, C. H., Shi, Q. J., & Ma, C. H. (2009). Preparation of different molecular weight polysaccharides from Porphyridium cruentum and their antioxidant activities. *International Journal of Biological Macromolecules*, *1*, 42–47.
Wang, D. F., Wang, C. H., Li, J., & Zhao, G. W. (2001). Components and activity of polysaccharides from coarse tea. *Journal of Agricultural and Food Chemistry*, *49*, 507–510.
Yang, Z., Xu, Y., Jie, G., He, P., & Tu, Y. (2007). Study on the antioxidant activity of tea flowers (*Camellia sinensis*) Asia Pacific. *Journal of Clinical Nutrition*, *16*, 148–152.
Zamora, F., Gonzalez, M. C., Duenas, M. T., Irastorza, A., Velasco, S., & Ibarburu, I. (2002). Thermo degradation and thermal transitions of an exopolysaccharide produced by Pediococcus damnosus 2.6. *Journal of Macromolecular Science: Physics*, *41*, 473–486.
Zhang, M., Cui, S. W., Cheung, P. C. K., & Wang, Q. (2007). Antitumor polysaccharides from mushrooms: A review on their isolation process, structural characteristics and antitumor activity. *Trends in Food Science & Technology*, *18*, 4–19.
Zhang, Y. Y., Li, S., & Zhang, L. N. (2010). Aggregation behavior of triple helical polysaccharide with low molecular weight in diluted aqueous solution. *The Journal of Physical Chemistry B*, *114*, 4950–4954.
Zhou, J., Ding, J. P., & Wang, Z. N. (1997). Effect of tea polysaccharides on blood-glucose, blood lipid and immunological function of mice. *Journal of Tea Science*, *17*, 75–79.